



Cite this: RSC Adv., 2017, 7, 32229

Competitive biosorption behavior of Pt(IV) and Pd(II) by *Providencia vermicola*

Hang Xu,^a Ling Tan,^{ID}^a Haigang Dong,^b Jia He,^a Xinxing Liu,^a Guanzhou Qiu,^a Qianfeng He^{cd} and Jianping Xie^{*a}

Biosorption is an effective way to recover or remove metal ions from wastewater; however, the biosorption process in a multiple metal ion solution is still unclear. In this paper, we investigated the simultaneous biosorption in a Pt(IV) and Pd(II) binary system using *Providencia vermicola*. Kinetics, isotherms, thermodynamics, TEM, and FT-IR were carried out to elucidate the competition behavior and adsorption mechanisms in the process. The results revealed that Pd(II) had a relevant effect on the Pt(IV) biosorption, but the interference of Pt(IV) on the adsorption of Pd(II) was considerably less intense. The maximum adsorption capacity of *P. vermicola* was 30.20 mg g^{-1} for Pt(IV) and 119.00 mg g^{-1} for Pd(II) in the binary system, which corresponded to 3.94 times larger selective adsorption toward Pd(II). The TEM results revealed that *P. vermicola* could adsorb Pt(IV) and Pd(II) both extracellularly and intracellularly. The FT-IR results indicated that amine groups played major roles in adsorbing Pt(IV), but amine, carboxyl, hydroxyl, and phosphate groups were critical to adsorb Pd(II). This study demonstrates that *P. vermicola* is a promising biosorbent and could selectively adsorb Pd(II) in the Pt(IV)–Pd(II) binary system.

Received 7th March 2017
Accepted 5th June 2017

DOI: 10.1039/c7ra02786a
rsc.li/rsc-advances

1. Introduction

Biosorption is a promising technology for the removal and recovery of metals from waste solutions, because of its low-cost, high effectiveness at low concentrations, and environmentally friendly nature.^{1–4} The removal of the metal ions by biomass can occur through any or a combination of natural chemical mechanisms such as ion exchange, complexation, chelation, and precipitation.^{5–7}

Nevertheless, biosorption has not been applied in practical industrial processes.⁸ A major reason is that the adsorption capacities of most biosorbents are not very high.^{9,10} Another great challenge is that single metal species rarely exist in the natural streams and industrial wastewater.^{11,12} Therefore, more effective and selective adsorbents are needed to be developed.^{10,13} Meanwhile, it is necessary to evaluate the simultaneous biosorption behavior and interactions of two or more metal species.¹⁴

There are three possible interactive effects of a mixture of metal ions: synergism, antagonism, and non-interaction. Aksu

*et al.*¹⁵ studied binary adsorption of iron(II) and iron(III)–cyanide complex ions on *Rhizopus arrhizus*. The results showed the combined action of two components was synergistic. Mahamadi *et al.*¹¹ used *Eichhornia crassipes* to adsorb Pb²⁺, Cd²⁺, and Zn²⁺ in binary and ternary systems. It showed that the combined effect among the three metals was antagonistic, and the metal adsorption followed the order: Pb²⁺ > Cd²⁺ > Zn²⁺. Meanwhile, the interactions between metal ions and adsorption sites were also reported. Sok Kim¹⁶ investigated selective adsorption behavior of *E. coli* in Pt(IV)–Pd(II) binary solution. Results showed that primary amines were the binding sites for Pt(IV) and Pd(II), and had higher affinity toward Pd(II).

Despite significant achievements in the multiple biosorption, the interactions between metal ions and functional groups in cell surface are still unclear. Therefore, this study investigated the adsorption properties and mechanisms of Pt(IV) and Pd(II) in bicomponent solutions by *P. vermicola*. Kinetic, isothermal, and thermodynamic models were applied to evaluate the competitive behavior of Pt(IV) and Pd(II). Furthermore, transmission electron microscopy (TEM) and fourier transform infrared spectroscopy (FT-IR) was performed to explore the competitive biosorption mechanisms of Pt(IV) and Pd(II).

2. Materials and methods

2.1. Materials

The *P. vermicola* strain was isolated from YueLu Mountain (Changsha, China). The microorganism was cultivated in Lysogeny Broth medium at 30 °C for 24 h. The biomass was

^aSchool of Minerals Processing and Bioengineering, Central South University, Changsha, 410083, China. E-mail: Xiejianping@csu.edu.cn; Fax: +86-0731-88836943; Tel: +86-0731-88836943

^bState Key Laboratory of Advanced Technologies for Comprehensive Utilization of Platinum Metals, Kunming Institute of Precious Metals, Kunming, 650106, China

^cSchool of Chemistry and Chemical Engineering, Central South University, Changsha, 410083, China

^dHunan Yonker Research Institute of Environmental Protection Co., Ltd, Changsha, 410330, China



collected by centrifugation at 10 000 rpm for 10 min. The 500 mg L⁻¹ of Pt(IV) and Pd(II) stock solutions were prepared by dissolving PtCl₄ or PdCl₂ in 0.1 M hydrochloric acid.

2.2. Adsorption experiments

For comparison of adsorption behavior of Pt(IV) and Pd(II), 0.40 g of wet biomass (equaled to 0.075 g dry biomass) was added to 50 mL of metal solution. The ratios of the metal concentrations (Pt(IV) : Pd(II)) were adjusted to about 1 : 1 (Pt(IV) : Pd(II) = 85.13 : 92.64 mg L⁻¹), about 2 : 1 (Pt(IV) : Pd(II) = 170.26 : 92.64 mg L⁻¹), and about 3 : 1 (Pt(IV) : Pd(II) = 255.39 : 92.64 mg L⁻¹). The biomass-containing solutions were stirred for 3 h at 170 rpm, 30 °C, and pH 4.0.

Binary adsorption kinetics: the initial concentrations of Pt(IV) and Pd(II) were 86.67 and 97.10 mg L⁻¹, respectively. The mixture was stirred at 170 rpm and 30 °C. The samples were collected at predetermined time intervals for analysis.

Binary isotherm adsorption: the initial concentrations of Pt(IV) and Pd(II) were adjusted to 50, 100, 200, 300, and 400 mg L⁻¹. The mixtures were stirred for 3 h at 170 rpm, 30 °C, and pH 4.0.

Binary thermodynamics: the initial concentrations of Pt(IV) and Pd(II) were 90.08 and 109.5 mg L⁻¹. The mixture was stirred for 3 h at 30 °C, 40 °C, and 50 °C, respectively.

The initial and final concentrations of Pt(IV) and Pd(II) were determined by Inductively Coupled Plasma Optical Emission Spectrometer (ICP-OES). The adsorption capacities of the metals on the biosorbent were calculated as follows:¹⁷

$$q_e = \frac{(C_0 - C_e)V}{M} \quad (1)$$

where C_0 and C_e (mg L⁻¹) are the initial and final concentrations of metal ions, V (L) is the working volume, and M (g) is the dry weight of biomass.

2.3. Transmission electron microscopy (TEM) and fourier transform infrared spectroscopy (FT-IR)

The precipitates of Pt(IV) and Pd(II) were characterized by TEM. After the biosorption experiment was finished, the bacterial suspension was washed three times with distilled water. The ultrathin sections of biomass samples were obtained using an ultramicrotome and then placed onto a copper grid. Finally, the samples were observed using a JEM-2100F transmission electron microscopy at 200 kV.

The functional groups of *P. vermicola* were identified by FT-IR. The spectra were recorded within the range of 4000–400 cm⁻¹ with samples prepared as KBr discs.

3. Results and discussion

3.1. Binary biosorption of *P. vermicola*

To compare adsorption behavior of Pt(IV) and Pd(II), binary batch experiments with different initial concentration ratios were carried out. When initial concentration ratio (Pt(IV) : Pd(II)) was 1 : 1, the adsorption capacity of Pd(II) (46.92 mg g⁻¹) was almost 3 times to that of Pt(IV) (17.83 mg g⁻¹); when the ratio was 2 : 1, the adsorption capacity of Pd(II) (44.19 mg g⁻¹) was

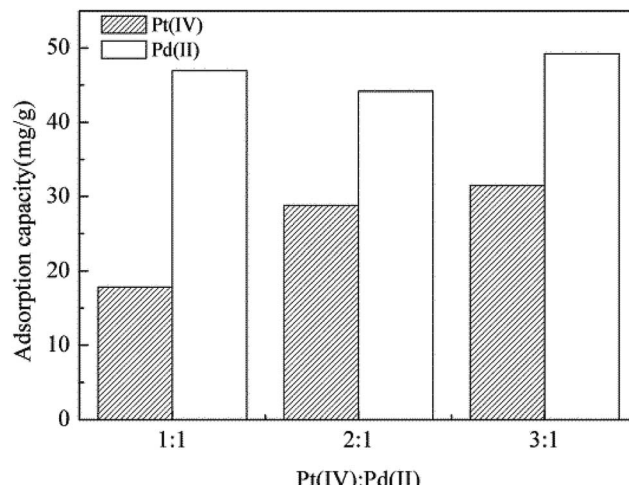


Fig. 1 Adsorption capacities of Pt(IV) and Pd(II) by *P. vermicola* in different binary systems. Initial concentration of Pt(IV) and Pd(II) in binary system: Pt(IV) = 85.13 mg L⁻¹ and Pd(II) = 92.64 mg L⁻¹ (Pt : Pd = 1 : 1); Pt(IV) = 170.26 mg L⁻¹ and Pd(II) = 92.64 mg L⁻¹ (Pt : Pd = 2 : 1); Pt(IV) = 255.39 mg L⁻¹ and Pd(II) = 92.64 mg L⁻¹ (Pt : Pd = 3 : 1).

about 2 times to that of Pt(IV) (28.82 mg g⁻¹); even when the ratio was 3 : 1, the adsorption capacity of Pd(II) (49.22 mg g⁻¹) was still higher than that of Pt(IV) (31.51 mg g⁻¹) (Fig. 1). These results showed that in the Pt(IV)-Pd(II) binary system, *P. vermicola* preferred to adsorb Pd(II).

Compared to the three different ratios, it showed that the adsorption capacity of Pd(II) was almost unchanged, while the adsorption capacity of Pt(IV) increased with increasing of the initial concentration of Pt(IV). These results suggested that the existence of Pt(IV) did not influence the adsorption of Pd(II), which implied the mechanisms of Pt(IV) and Pd(II) adsorption by *P. vermicola* was different.

3.2. Adsorption kinetics

The kinetic experiment was carried out not only to estimate the equilibrium time but also to investigate the controlling step and mechanism of the adsorption process.¹⁸ It was observed that the adsorption process was very rapid at the first 30 minutes, which could attribute to an initial non-special adsorption process between biomass and metal ions. And then reached the equilibrium slowly at around 3 h for both Pt(IV) and Pd(II), which were identified as a chemical sorption process such as covalent bonding or microprecipitation.¹⁹

The experimental data were described by linear pseudo-first-order and linear pseudo-second-order models. These models were expressed as follows:

Linear pseudo-first-order model:

$$\ln(q_e - q_t) = \ln q_e - k_1 t \quad (2)$$

Linear pseudo-second-order model:

$$\frac{t}{q_t} = \frac{1}{k_2 q_e^2} + \frac{t}{q_e} \quad (3)$$



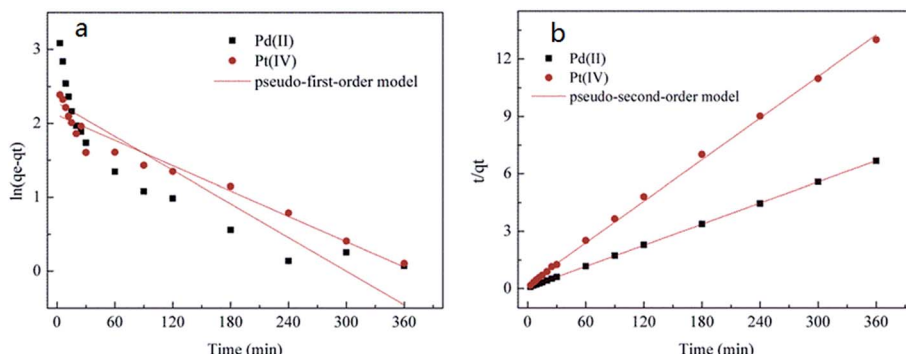


Fig. 2 Adsorption kinetics of the *P. vermicola* in the binary system: the fitted curve of the pseudo-first-order model (a) and pseudo-second-order model (b). Initial concentrations of Pt(iv) and Pd(II) were 86.67 mg L⁻¹ and 97.1 mg L⁻¹, respectively.

Table 1 The parameters of the kinetic models in binary adsorption

	Pseudo-first-order model			Pseudo-second-order model		
	q_e	K_1	R^2	q_e	K_2	R^2
Pt	8.28	0.0057	0.94	27.61	0.16	0.99
Pd	9.77	0.0076	0.80	54.29	0.34	0.99

where q_t is the adsorption amount of metal ion at time t (mg g⁻¹), q_e is the adsorption amount of metal ion at the equilibrium state (mg g⁻¹), k_1 is the first-order equilibrium rate constant (min⁻¹), k_2 is the second-order equilibrium rate constant (g mg⁻¹ min⁻¹).

Fig. 2 showed the kinetic models for Pt(iv) and Pd(II) adsorption, and kinetic parameters were presented in Table 1. From Table 1, the correlation coefficients (R^2) of the pseudo-second-order model for Pt(iv) and Pd(II) were higher than that of pseudo-first-order model. Moreover, the fitted curve of the pseudo-second-order model showed better agreement with the experimental data. Therefore, the pseudo-second-order model was more fitted with the adsorption process of Pt(iv) and Pd(II). This demonstrated that the controlling step might be chemical adsorption, but not mass transfer in solution.²⁰ The adsorption process may also involve valence forces through sharing electrons between biomass and metal ions.^{18,21}

In the case of the pseudo-second-order model, the estimated equilibrium uptake (q_e) values were 27.61 mg g⁻¹ for Pt(iv) and 54.29 mg g⁻¹ for Pd(II). The equilibrium rate constants (k_2) were 0.16 g mg⁻¹ min⁻¹ for Pt(iv) and 0.34 g mg⁻¹ min⁻¹ for Pd(II). Both q_e and k_2 of Pd(II) were higher than those values of Pt(iv). These results confirmed that *P. vermicola* could selectively bind with Pd(II).

3.3. Adsorption isotherm

Isotherm adsorption experiments were carried out to calculate the maximum adsorption capacity and evaluate the affinity in the bicomponent condition.

The linear Langmuir model, linear Freundlich model, and linear Langmuir competitive model (LCM) were applied to Pt(iv)

and Pd(II) isotherm data. These models were expressed as follows:

Linear Langmuir model:

$$\frac{C_e}{q_e} = \frac{1}{q_m} C_e + \frac{1}{q_m b} \quad (4)$$

Linear Freundlich model:

$$\ln q_e = \ln K_F + \frac{1}{n} \ln C_e \quad (5)$$

Linear LCM:

$$\frac{C_{e,1}}{C_{e,2} q_{e,1}} = \frac{C_{e,1}}{q_{m,1} C_{e,2}} + \frac{K_{L,2}}{K_{L,1} q_{m,1}} \quad (6)$$

where q_e is the amount of adsorbed metal (mg g⁻¹), C_e is the concentration of metal ion at equilibrium (mg L⁻¹), q_m is the maximum adsorption capacity (mg g⁻¹), b is the Langmuir constant (L mg⁻¹), K_F is the Freundlich constant related to adsorption capacity, n is the Freundlich constant.

The linear curves of three isotherm models were shown in Fig. 3, and isotherm parameters were presented in Table 2. The results showed that the correlation coefficients of Langmuir were 0.97 for Pt(iv) and 0.95 for Pd(II), which were higher than those values of other isotherm models. Therefore, the experimental data of Pt(iv) and Pd(II) adsorption in binary system could fit best to the Langmuir isotherm model. This indicated that a monolayer adsorption process might dominate the present adsorption process rather than a multiple adsorption one.¹⁸

In the case of the LCM model, we found that the Pt(iv) adsorption process could be described well, but the Pd(II) adsorption process did not. Because the value of $K_{L,2}/K_{L,1}$ was negative, which was irrational. These results probably implied that the presence of Pd(II) caused competitive effect on Pt(iv) sorption, while Pt(iv) hardly influenced the Pd(II) adsorption in binary system.

Isotherm model constants, which express the surface properties and affinity of the biosorbent, can be used to compare the biosorption capacity of biomass for different



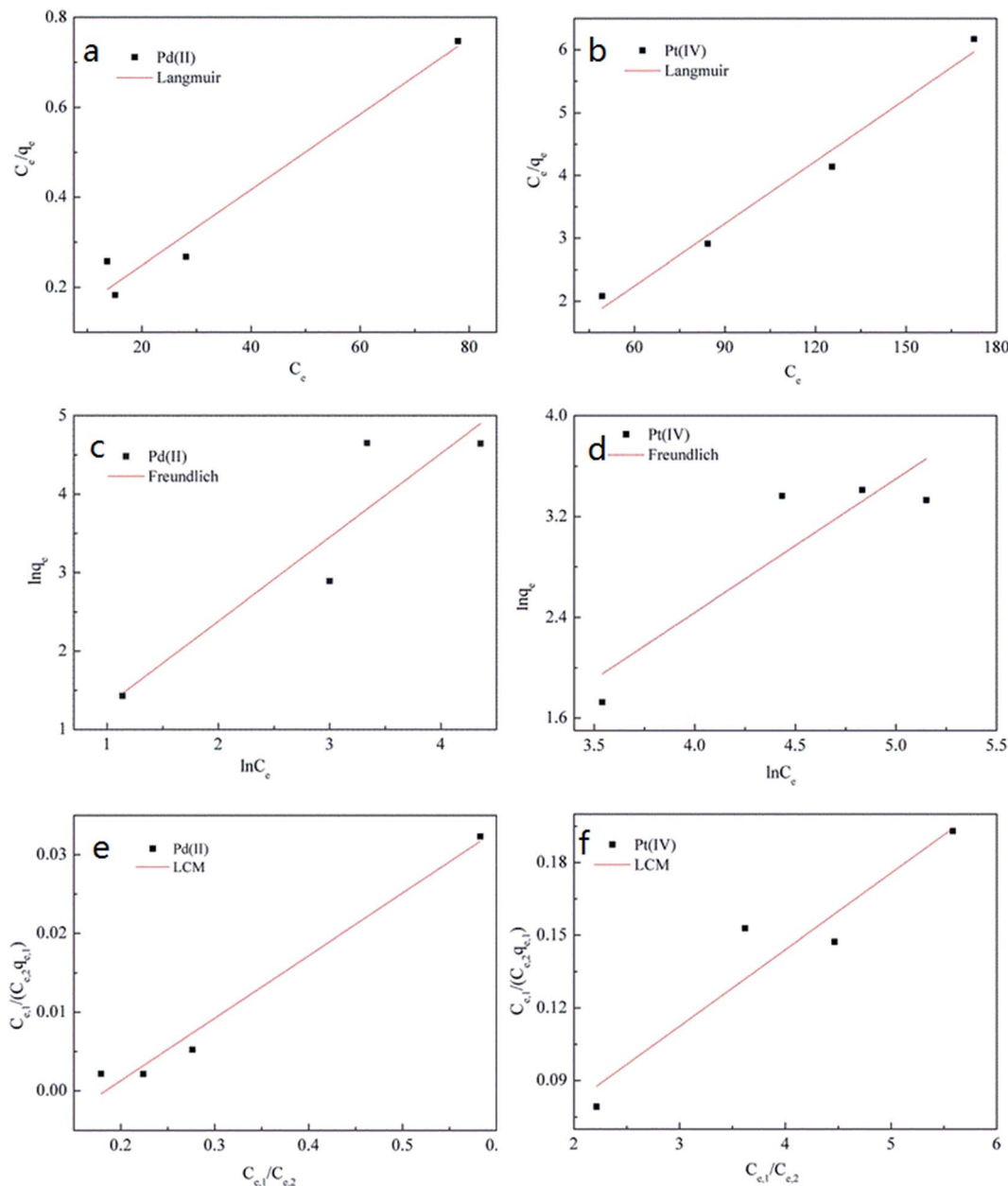


Fig. 3 Isotherms of Pt(IV) and Pd(II) by *P. vermicola* in the binary system: the fitted curves of the Langmuir (a and b), Freundlich (c and d), and LCM (e and f).

Table 2 The parameters of the Langmuir, Freundlich, and LCM in binary adsorption

	Langmuir				Freundlich			LCM		
	$q_e/(\text{mg g}^{-1})$	$q_{\text{max}}/(\text{mg g}^{-1})$	$b/(\text{L mg}^{-1})$	R^2	K_F	$1/n$	R^2	$q_{\text{max}}/(\text{mg g}^{-1})$	$K_{L,2}/K_{L,1}$	R^2
Pt	30.30	30.20	0.13	0.97	0.16	1.06	0.72	31.64	0.56	0.86
Pd	105.10	119.00	0.10	0.95	1.27	1.07	0.78	12.58	-0.18	0.97

adsorbate.²² One of the most important parameters is the maximum adsorption capacity. According to the Langmuir model, the maximum adsorption capacity of Pd(II) (119.00 mg

g⁻¹) was higher than that of Pt(IV) (30.20 mg g⁻¹). This could be another evidence to prove that *P. vermicola* had greater affinity to Pd(II) than Pt(IV).

Table 3 The parameters of the thermodynamic model in binary adsorption

	$T/^\circ\text{C}$	$\Delta G^0/(\text{kJ mol}^{-1})$	$\Delta H^0/(\text{kJ mol}^{-1})$	$\Delta S^0/[\text{J}(\text{K mol})^{-1}]$	R^2
Pt	20	-0.09	14.98	49.54	0.91
	30	-0.42			
Pd	40	-1.12	6.67	38.54	0.47
	20	-4.94			
	30	-5.55			
	40	-5.71			

3.4. Adsorption thermodynamics

The thermodynamic parameters, including Gibbs free energy change (ΔG^0), enthalpy change (ΔH^0), and entropy change (ΔS^0), were shown in Table 3. The negative values of ΔG^0 demonstrated the spontaneous nature of Pt(iv) and Pd(ii) adsorption by *P. vermicola* in binary system. The positive values of ΔH^0 reflected that the present adsorption was endothermic and might exist strong bonding between metal ions and biosorbent. The positively values of ΔS^0 reflected the increased randomness at the solid–solution interface during the biosorption of Pt(iv) and Pd(ii) onto *P. vermicola*.^{22,23}

3.5. TEM analysis

The ultrathin sections of bacteria were investigated to identify the presence, spatial distribution, and morphology of Pt(iv) and Pd(ii) precipitates by TEM.²⁴ As shown in Fig. 4, the *P. vermicola* could sequester Pt(iv) and Pd(ii) both extracellularly and intracellularly. After Pt(iv) and Pd(ii) uptake for 3 h, numerous small particles were distributed uniformly on the cell wall. At the same time, a certain amount of precipitates could be observed in the cell, which clustered together to bigger agglomerates. It was possible that intracellular precipitates were isolated in particular area or bound to intracellular proteins in the cytoplasm.²⁵

Palladium precipitates were formed in a previous study by *P. vermicola*, which showed similarities with our results.²⁶ Kevin Deplanche *et al.*²⁷ revealed that the Pd(0) particles were located on both sides of the cytoplasmic membrane using *E. coli* mutant

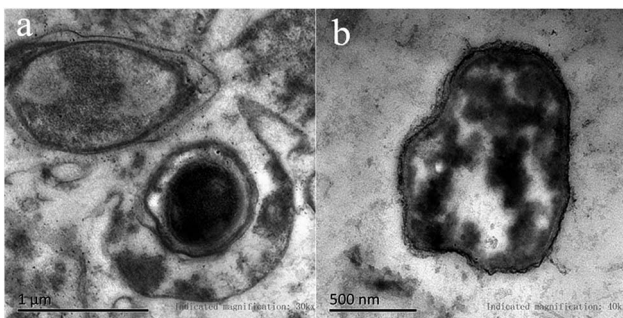


Fig. 4 TEM analysis of *P. vermicola* before and after adsorption: (a) image of blank biomass; (b) image of metal-loaded biomass after 3 h of biosorption in Pt(iv) and Pd(ii) binary system.

strains, which involved in the Pd(ii) reduction process of the particular hydrogenases. Synthia Maes *et al.*²⁸ also reported that both intra- and extracellular platinum precipitates were formed using halophilic bacteria. Therefore, the bacterial interaction in these biosorption processes is believed to consist of two steps: (1) the initial adsorption of metal ions to the cell, which is followed by (2) the transportation of the adsorbed metal ions into the cytoplasm, and gradually formed complexes.^{26,29}

3.6. FT-IR analysis

To evaluate possible reactions between metal ions and surface functional groups, the FT-IR spectra of *P. vermicola* before and after adsorption were recorded. As shown in Fig. 5a, the strong and broad band around 3421.38 cm^{-1} represented the stretching of the N–H and O–H of the amine groups. The peak at 1650.11 cm^{-1} indicated C=O stretching in the amide I bond of peptides. The peak around 1542.25 cm^{-1} was assigned to N–H bending and C–N stretching in amide II bond of peptides. The peak around 1396.88 cm^{-1} was caused by C–O stretching from carboxyl. The band at 1236.32 cm^{-1} resulted from the stretching vibration of P=O of phosphate. The peak around 1079.37 cm^{-1} can be attributed to stretching vibration of C–O and P–O from peptidoglycan.^{30–32} The results of FT-IR suggested that *P. vermicola* possessed many surface functional groups such as nitrogen-, oxygen- and phosphoryl-containing groups.

After Pt(iv) adsorption (Fig. 5b), the peak at 3421.38 cm^{-1} shifted to 3430.34 cm^{-1} , which indicated that amine groups played important roles in adsorbing Pt(iv). The shifts of the peaks at 1650.11 cm^{-1} and 1542.25 cm^{-1} showed that amide I and amide II bonds were also involved in binding with Pt(iv). After Pd(ii) adsorption (Fig. 5c), the shifts of the peaks from 1396.88 cm^{-1} to 1386.59 cm^{-1} and from 1386.59 cm^{-1} to 1069.34 cm^{-1} suggested that P=O and C–O or P–O groups played major roles in adsorbing Pd(ii). Amine and phosphate groups were also engaged because of the slight shifts of the peaks at 1542.25 cm^{-1} and 1236.32 cm^{-1} . From Fig. 5d, the FT-IR spectrum of binary adsorption was similar to that of Pd(ii)

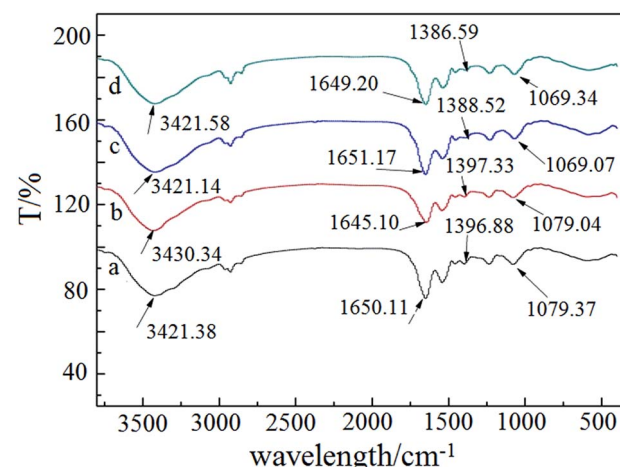


Fig. 5 FT-IR spectra of the *P. vermicola* (a), Pt adsorption (b), Pd adsorption (c), binary adsorption (d).



adsorption. The peaks, which largely shifted, were almost associated with Pd(II) adsorption. The shifts of the peaks, which related to Pt adsorption, were not obvious.

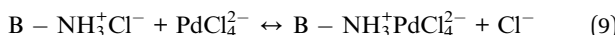
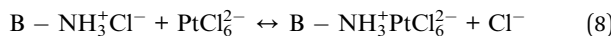
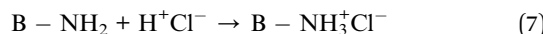
These results verified that the surface functional groups of *P. vermicola* binding Pt(IV) and Pd(II) might have several differences. Nitrogen-containing groups played major roles in adsorbing Pt(IV), and nitrogen-, oxygen- and phosphoryl-containing groups were critical to adsorb Pd(II).

3.7. Adsorption mechanisms

In order to explain the differences of Pt(IV) and Pd(II) adsorption behavior by *P. vermicola*, it is useful to consider the possible adsorption mechanisms. PH is one of the most important factors to influence the biosorption process, because pH could affect not only the solution chemistry of metal ions, but also site dissociation of the cell surface.³³

At pH 4.0, when the chloride concentration is high (>10 mmol dm⁻³), platinum should be found as PtCl₆²⁻, and the predominant species of palladium are PdCl₄²⁻ and hydroxyl complexes such as Pd(OH)⁺, Pd(OH)₂ or Pd(OH)₄.²⁻³⁴ In addition, The pK_a values are 7-10 for amine groups and 4.8 for carboxyl groups in the cell wall.^{34,35} Therefore, neutral amine groups and acidic carboxyl groups were protonated under the experimental conditions.

According to these, electrostatic attraction and anion exchange might play important roles to adsorb metal ions. Positive amine groups could bind anionic metal-chloride complex ions by electrostatic attraction. Anionic metal-chloride complex ions could be bound to the cell wall by anion exchange mechanism as below.¹⁶



Except electrostatic attraction and anion exchange mechanism, another mechanism might be also involved in Pd(II) sorption. For example, Pd(OH)⁺ was possibly bound to carboxyl groups by exchanging with hydrogen ions. In addition, hydroxyl and phosphate groups could bind palladium complexes through complexation or chelation.³⁴ Phosphate groups might be also engaged in modification of the extracellular protein.

As a result, the mechanisms of Pt(IV) adsorption were mainly electrostatic attraction and anion exchange. Pd(II) adsorption could be achieved by electrostatic attraction, anion and cation exchange, complexation and chelation. The difference of adsorption mechanisms could be a reason for selectively adsorbing Pd(II) by *P. vermicola*.

4. Conclusions

This study explored the biosorption properties and mechanisms of Pt(IV) and Pd(II) onto *P. vermicola* in binary system.

(1) In Pt(IV)-Pd(II) binary system, *P. vermicola* preferred to adsorb Pd(II); furthermore, the presence of Pt(IV) could hardly influence on Pd(II) biosorption.

(2) Kinetic and isotherm models confirmed that *P. vermicola* had greater affinity to Pd(II) and selectively adsorbed Pd(II). Chemical adsorption was the controlling step of the adsorption process.

(3) The mechanism of Pd(II) adsorption was more complicated than that of Pt(IV). Amine groups were important to both Pt(IV) and Pd(II) adsorption. In addition, carboxyl, hydroxyl, and phosphate groups were also involved in Pd(II) adsorption. It was a main reason for selectively adsorbing Pd(II) onto *P. vermicola* in Pt(IV)-Pd(II) binary system.

In conclusion, *P. vermicola* could be used as an effective biosorbent to recover Pd(II) in a mixture solution of Pt(IV) and Pd(II). This study could also provide theoretical guidance for the treatment of multiple industrial wastewater.

Acknowledgements

This work was supported by the National Natural Science Foundation of China (51104189), the 53rd China Postdoctoral Science Foundation (2013M531814), the China Postdoctoral Science Foundation (2015T80880), and the State Key Laboratory of Advanced Technologies for Comprehensive Utilization of Platinum Metals (SKL-SPM-201508).

References

- 1 J. Park, S. W. Won, J. Mao, I. S. Kwak and Y. S. Yun, *J. Hazard. Mater.*, 2010, **181**, 794-800.
- 2 A. Mishra, B. D. Tripathi and A. K. Rai, *Ecotoxicol. Environ. Saf.*, 2016, **132**, 420-428.
- 3 Z. Chen, X. Pan, H. Chen, Z. Lin and X. Guan, *World J. Microbiol. Biotechnol.*, 2015, **31**, 1729-1736.
- 4 E. Alipanahpour Dil, M. Ghaedi, G. R. Ghezelbash, A. Asfaram and M. K. Purkait, *J. Ind. Eng. Chem.*, 2017, **48**, 162-172.
- 5 F. Veglio and F. Beolchini, *Hydrometallurgy*, 1997, **44**, 301-316.
- 6 S. W. Won, P. Kotte, W. Wei, A. Lim and Y. S. Yun, *Bioresour. Technol.*, 2014, **160**, 203-212.
- 7 S. W. Won, J. Park, J. Mao and Y. S. Yun, *Bioresour. Technol.*, 2011, **102**, 3888-3893.
- 8 X. Ju, K. Igarashi, S. Miyashita, H. Mitsuhashi, K. Inagaki, S. Fujii, H. Sawada, T. Kuwabara and A. Minoda, *Bioresour. Technol.*, 2016, **211**, 759-764.
- 9 C. P. Okoli, P. N. Diagboya, I. O. Anigbogu, B. I. Olu-Owolabi and K. O. Adebawale, *Environ. Earth Sci.*, 2017, **76**, 33.
- 10 A. Asfaram, M. Ghaedi, G. R. Ghezelbash and F. Pepe, *Ecotoxicol. Environ. Saf.*, 2017, **139**, 219-227.
- 11 C. Mahamadi and T. Nharingo, *Bioresour. Technol.*, 2010, **101**, 859-864.
- 12 Y. Sağ and T. Kutsal, *Process Biochem.*, 1996, **31**, 561-572.
- 13 W. Wei, S. Lin, D. H. Reddy, J. K. Bediako and Y. S. Yun, *J. Hazard. Mater.*, 2016, **318**, 79-89.



14 L. Li, F. Liu, X. Jing, P. Ling and A. Li, *Water Res.*, 2011, **45**, 1177–1188.

15 Z. Aksu and H. Gülen, *Process Biochem.*, 2002, **38**, 161–173.

16 S. Kim, M. H. Song, W. Wei and Y. S. Yun, *J. Hazard. Mater.*, 2015, **283**, 657–662.

17 H. Xie, Q. Zhao, Z. Zhou, Y. Wu, H. Wang and H. Xu, *RSC Adv.*, 2015, **5**, 33478–33488.

18 K. Fujiwara, A. Ramesh, T. Maki, H. Hasegawa and K. Ueda, *J. Hazard. Mater.*, 2007, **146**, 39–50.

19 C. L. Mack, B. Wilhelm, J. R. Duncan and J. E. Burgess, *Miner. Eng.*, 2008, **21**, 31–37.

20 Y. S. Ho and G. Mckay, *Process Biochem.*, 1999, **34**, 451–465.

21 A. Özer, D. Özer and H. İ. Ekiz, *Adsorption*, 2005, **10**, 317–326.

22 G. Uslu and M. Tanyol, *J. Hazard. Mater.*, 2006, **135**, 87–93.

23 S. Muthusamy and S. Venkatachalam, *RSC Adv.*, 2015, **5**, 45817–45826.

24 S. Maes, R. Props, J. P. Fitts, R. D. Smet, R. Vilchezvargas, M. Vital, D. H. Pieper, F. Vanhaecke, N. Boon and T. Hennebel, *Environ. Sci. Technol.*, 2016, **50**, 2619.

25 J. Bai, X. Yang, R. Du, Y. Chen, S. Wang and R. Qiu, *J. Environ. Sci.*, 2014, **26**, 2056–2064.

26 L. Tan, H. Dong, X. Liu, J. He, H. Xu and J. Xie, *RSC Adv.*, 2017, **7**, 7060–7072.

27 K. Deplanche, I. Caldelari, I. P. Mikheenko, F. Sargent and L. E. Macaskie, *Microbiology*, 2010, **156**, 2630.

28 S. Maes, R. Props, J. P. Fitts, S. R. De, R. Vilchezvargas, M. Vital, D. Pieper, F. Vanhaecke, N. Boon and T. Hennebel, *Environ. Sci. Technol.*, 2016, **50**, 2619.

29 S. Maes, R. Props, J. P. Fitts, R. D. Smet, F. Vanhaecke, N. Boon and T. Hennebel, *PLoS One*, 2017, **12**, e0169093.

30 R. Aravindhan, F. Aafreen, M. Selvamurugan, J. Raghava Rao and U. N. Balachandran, *Clean Technol. Environ.*, 2011, **14**, 727–735.

31 J. Bai, X. Yang, R. Du, Y. Chen, S. Wang and R. Qiu, *Clean Technol. Environ. Policy*, 2014, **26**, 2056–2064.

32 Y.-G. Liu, T. Liao, Z.-B. He, T.-T. Li, H. Wang, X.-J. Hu, Y.-M. Guo and Y. He, *Trans. Nonferrous Met. Soc. China*, 2013, **23**, 1804–1814.

33 A. Esposito, F. Pagnanelli and F. Vegliò, *Chem. Eng. Sci.*, 2002, **57**, 307–313.

34 I. de Vargas, L. E. Macaskie and E. Guibal, *J. Chem. Technol. Biotechnol.*, 2004, **79**, 49–56.

35 J. B. Fein, C. J. Daughney, N. Yee and T. A. Davis, *Geochim. Cosmochim. Acta*, 1997, **61**, 3319–3328.

